Hydrogen Absorption into Copper-Coated Titanium Measured by In Situ Neutron Reflectometry and Electrochemical Impedance Spectroscopy

Situm, Arthur; Bahadormanesh, Behrouz; Bannenberg, Lars J.; Ooms, Frans; Feltham, Hunter A.; Popov, German; Behazin, Mehran; Goncharova, Lyudmila V.; Noël, James J.

DOI
10.1149/1945-7111/acc763

Publication date
2023

Document Version
Final published version

Published in
Journal of the Electrochemical Society

OPEN ACCESS

Hydrogen Absorption into Copper-Coated Titanium Measured by In Situ Neutron Reflectometry and Electrochemical Impedance Spectroscopy

To cite this article: Arthur Situm *et al* 2023 *J. Electrochem. Soc.* **170** 041503

Journal of The Electrochemical Society, 2023 **170** 041503

Hydrogen Absorption into Copper-Coated Titanium Measured by In Situ Neutron Reflectometry and Electrochemical Impedance Spectroscopy

Arthur Situm,[1] Behrouz Bahadormanesh,[1] Lars J Bannenberg,[2] Frans Ooms,[2] Hunter A Feltham,[1] Guerman Popov,[3] Mehran Behazin,[4] Lyudmila V Goncharova,[3] and James J Noël[1,z]

[1]*Department of Chemistry, Western University, London, ON, Canada*
[2]*Reactor Institute Delft, Delft University of Technology, Delft, The Netherlands*
[3]*Department of Physics, Western University, London, ON, Canada*
[4]*Nuclear Waste Management Organization, Toronto, ON, Canada*

One concern regarding the used nuclear fuel containers proposed for use in a Canadian deep geological repository (DGR) is the possibility that a small amount of hydrogen might be absorbed into their copper coating, potentially altering its mechanical properties. Reported herein is a study of hydrogen absorption into 50 nm of copper, coated on 4 nm of Ti using in situ neutron reflectometry (NR) and electrochemical impedance spectroscopy (EIS). NR results show that hydrogen is absorbed when the copper is cathodically polarized below the threshold for the hydrogen evolution reaction (HER), but that the hydrogen concentrates in the underlying titanium layer rather than concentrating in the copper coating. The hydrogen concentration in titanium rapidly rose when the HER was initiated and was observed to reach a steady state at $TiH_{1.5}$. Over the course of 55h of cathodic polarization, the concentration of hydrogen in the copper remained below the NR detection limit (2 at %). The portion of hydrogen atoms produced that diffused through the copper layer was initially 3.2%, suggesting a possible upper limit for hydrogen uptake by the copper coating of the UFC, although definitive conclusions can only be drawn from studies on 3 mm copper-coated steel samples.

 [DOI: 10.1149/1945-7111/acc763]

Manuscript submitted February 20, 2023; revised manuscript received March 22, 2023. Published April 6, 2023.

Supplementary material for this article is available online

Nuclear power is a valuable tool in the fight against climate change, due to its extremely low greenhouse gas emissions.[1] However, the complexities associated with implementing a long-term plan for the disposal of used nuclear fuel may limit the use of nuclear power.[2] In many countries, including Canada, Sweden and Finland, the plan for the permanent disposal of used nuclear fuel is to place it in a deep geological repository (DGR) within a multi-barrier system.[2,3] In Canada, implementing the multi-barrier system will involve loading the used fuel bundles into carbon steel containers coated with 3 mm of copper (applied mostly using electrodeposition but with a small amount of coldspray deposition).[3] These copper-coated used fuel containers (UFCs) will then be placed within bentonite clay buffer boxes to limit the penetration of groundwater and cationic species to the UFC surface.[3] Finally, the bentonite buffer boxes will be placed deep underground within a suitable host rock, selected based on favourable chemical and geological characteristics.[3]

An aspect of the disposal plan that has received significant attention is the possibility of hydrogen absorption into the copper coatings and what effect this will have on the properties of the copper.[4–8] Hydrogen absorbed into copper can become trapped at grain boundaries, dislocations and other crystalline imperfections, potentially creating hydrogen-filled microvoids.[9,10] Molecular dynamic (MD) simulations of hydrogen dissolved in the lattice of copper indicate that hydrogen stabilizes the formation of vacancy clusters, which may result in void formation by impurities within the copper, such as oxygen, potentially resulting in the degradation of copper's ductility.[11] While a drop in creep ductility is observed during electrochemical charging of hydrogen into copper, a failure of the Canadian UFC through creep is not possible due to the copper being applied directly to the load-bearing steel container and thus not experiencing tensile stress.[3,8] Concerns have also been raised about the possibility of stress corrosion cracking (SCC) of the copper in the presence of HS^-, although SCC is considered very unlikely to occur, due to the low concentrations of HS^- predicted to reach the surface of the UFC.[3,4,12] Lastly, although the possibility of hydrogen embrittlement, hydrogen blistering, and copper coating debonding is low due to the low solubility of hydrogen in copper, it is still necessary to study further the behaviour and impact of hydrogen in copper within DGR-relevant conditions.[3,13]

A series of studies have been conducted to examine the effect of hydrogen absorption into copper.[5–8] Many of these studies have been focused on the oxygen-free, phosphorus-doped (OFP) copper proposed for use in the Swedish and Finnish dual-walled copper/cast-iron UFCs (the alloyed phosphorus is used to impart the tolerance to deformation necessary to mitigate creep in the dual-walled design).[3] With this approach, water radiolysis and corrosion of the copper by hydrosulphide (HS^-) ions are considered the two routes most likely to generate hydrogen that could be absorbed into the copper coating, although many studies employ electrochemical charging as a way of controlling the generation of hydrogen.[3,4]

Yagodzinskyy et al. performed continuous electrochemical charging of hydrogen into OFP copper and found a reduction in the creep rate and decreased tensile strength, although the hydrogen buildup in the copper was not measured in this study.[8] Yagodzinskyy et al. added 10mg l^{-1} of $NaAsO_2$ to the electrolyte to inhibit hydrogen recombination, thereby increasing the absorption of hydrogen into the copper.[8,10] Using an As(III) species or thiourea as a hydrogen recombination inhibitor to induce hydrogen absorption into copper is the standard procedure for cathodic charging; however, this causes the rate of hydrogen absorption into copper to be unrealistically high.[14] Similarly, Martinsson et al. performed continuous electrochemical charging of OFP copper under aggressive conditions, with the hydrogen content in OFP copper increasing from 0.6 to almost 100 wt. ppm after three weeks.[7] This study showed that even under these aggressive conditions, the penetration of hydrogen was less than 100μm, suggesting that a debonding of the UFC's copper coating would be unlikely, as the hydrogen's low solubility in copper would limit its diffusion to the Cu-steel interface.[3,7] Sahiluoma et al. performed cathodic charging of OFP copper that has an increased

[z]E-mail: jjnoel@uwo.ca

oxygen content due to being welded in air rather than an inert gas.[15] Using thiourea as a hydrogen recombination inhibitor, hydrogen-induced void formation was observed near the copper surface.[15]

Lousada et al. claimed that γ-radiolysis of deoxygenated water may induce hydrogen absorption into copper as a result of the radiolytic formation of hydrogen atoms at the copper/water interface.[6] However, they did not report the background hydrogen concentration in the copper used in this work.[6] Moreover, the dose rate applied was 486 Gy h^{-1}, which is much higher than the expected dose rate at the Canadian UFC surface, which is estimated to start at ~1Gy h^{-1} at fuel encapsulation but will decay to 0.01 Gy h^{-1} after 200 years.[3,6] A higher dose rate would create higher concentrations of H_2 and $H^{\bullet}$, leading to increased hydrogen absorption; thus it is doubtful that the same effect would be observed at lower dose rates over longer periods, even if the same overall dose was applied. For example, Turnbull et al. examined corrosion that occurred on a section of copper piping used to carry 40 °C humid process air in Canada's now shut-down National Research Universal (NRU) reactor.[16] The copper sample experienced a γ radiation dose rate of approximately 0.015Gy h^{-1} over the course of 40 years. Although the low dose rate and negligible H_2 formation within the humid environment prevent a direct comparison,[11] Vickers microhardness measurements indicated that little to no irradiation hardening occurred to the irradiated pipe despite the constant γ and neutron irradiation during the operation of the NRU reactor, and no blistering was observed on the pipe, which would have been indicative of excess hydrogen absorption.[14] Currently, radiation experiments are being performed on copper samples immersed in water, the results of which will be the focus of a future study.

Forsström et al. studied the absorption of hydrogen into OFP copper samples induced by the corrosion of copper by HS^- in deoxygenated water at 90 °C.[5] These samples were simultaneously exposed to slow strain rate tensile (SSRT) testing to investigate the potential for SCC.[5] Hydrogen absorption in this case was due to the hydrogen evolution reaction (HER), which results from the cathodic reaction of the copper corrosion by HS^-.[5] This study used two different HS^- concentrations, 0.001 and 0.00001M, which are higher and lower, respectively, than the expected concentration at the Swedish DGR site in Forsmark (i.e., 0.00012M).[5] The results showed that, while the 0.001M HS^- increased the hydrogen in the OFP copper samples over that of the unreacted material, the samples exposed to 0.00001M HS^- saw a loss of hydrogen (or no significant change in absorbed hydrogen if also subjected to SSRT).[5] These results demonstrate that the absorption of hydrogen from HS^- exposure must be sufficient to counteract the spontaneous outgassing of hydrogen, if the concentration of hydrogen in copper is to remain constant.[5] A review of the thermodynamics of hydrogen outgassing from copper has been conducted by Hedin et al. in the context of copper's very limited corrosion in pure O_2-free water.[17] Additionally, the results of the SSRT testing are consistent with the hypothesis that tensile strain increases the number of lattice defects, creating additional sites to act as sinks for hydrogen.[5] While the authors did observe corrosion at grain boundaries, hydrogen embrittlement was not observed to have occurred, and the brittle copper sulphide films were not expected to be protective (a requirement for SCC and pitting).[5,18,19]

All studies listed that examined the concentration of hydrogen in copper samples have relied on ex situ methods for the analysis of hydrogen, either thermal desorption spectroscopy (TDS) or glow discharge optical emission spectrometry (GDOES).[5–7] While these techniques are either partially or fully destructive to the samples, neutron scattering techniques have been demonstrated to be adept at quantifying the presence of hydrogen in transition metals such as copper non-destructively.[20] Indeed, neutron reflectometry (NR) has previously been used for studying the corrosion and absorption of hydrogen into various metal substrates.[21] For example, Vezvaie et al. monitored the absorption of hydrogen into a 50 nm thick titanium film in situ, using NR and electrochemical impedance spectroscopy (EIS) recorded as a function of applied cathodic polarization.[22] These results showed that at potentials lower than −600mV vs the saturated calomel electrode (SCE) in neutral pH solution, both significant hydrogen absorption into the titanium film and the formation of TiH_X occurred.[22]

The current research aims to measure the absorption and permeation of hydrogen into copper, in situ, as a function of applied potential and time, to provide fundamental information on related potential adverse effects of hydrogen absorption on the copper coating; we accomplished this using a combination of NR and EIS. Additionally, hydrogen concentrations were measured as a function of applied potential in samples of OFP copper without any hydrogen recombination inhibitors.

To the best of the authors' knowledge, this is the first attempt to study the ingress of hydrogen into copper in situ. Similar to the aforementioned studies, this work used cathodic charging for hydrogen loading. A thin film of titanium was used as an adhesion layer between the copper thin film and the silicon wafer substrate. As titanium is known to readily absorb hydrogen to form titanium hydride, the detection of this using NR indicates the diffusion of hydrogen through the copper film, even if the hydrogen concentration in the copper film does not exceed the detection limit for hydrogen by NR (about 2 at %, or 324 wt. ppm). The work presented herein represents a preliminary study of hydrogen absorption into copper, using cathodic charging. Future studies examining the role of HS^- and γ radiation on hydrogen absorption are planned.

Experimental

Hydrogen measurements in cathodically polarized OFP copper.—OFP copper samples were cathodically charged in deoxygenated, mildly alkaline, saline solution to determine the potential at which hydrogen absorption initiates in the absence of a hydrogen recombination inhibitor. Samples of OFP copper provided by the Swedish Nuclear Fuel and Waste Management Co. (SKB) were cut into cubes (of 5 mm side length) with a threaded hole cut into one face. To remove any hydrogen that was initially present in the OFP copper, samples were annealed at 900 °C for 10min in a quartz tube under vacuum. The surfaces of the samples were then[1]: ground with 240, 600, 800, 1000, 1200, and 1500 grade SiC papers in succession (applied to all surfaces except the one with the threaded hole)[2]; sonicated in Type 1 water (filtered using a Thermo Scientific Barnstead Nanopure 7143 ultrapure water system, resistivity = 18.2 MΩ cm)[3]; sonicated in methanol (reagent grade)[4]; sonicated again in Type 1 water; and[5] dried under a jet of argon gas. Following surface preparation, a stainless-steel rod was inserted into the threaded hole of the OFP copper samples. Polytetrafluoroethylene (PTFE) tape was used to cover the stainless-steel rod and the face of the OFP copper with the threaded hole to avoid a bimetallic couple.

Experiments to induce the absorption of hydrogen into the samples were then conducted in a conventional three-electrode cell using a platinum plate counter electrode and an SCE as the reference electrode. Deoxygenated pH 9 0.1M NaCl solution was selected as the electrolyte to have the same NaCl concentration and similar pH to those used in previous studies examining the corrosion of copper in sulphide-containing solutions.[18,19,23] The pH 9, 0.1M NaCl electrolyte was prepared using Type 1 water and NaCl (NaCl, 99.0% assay) with pH adjustments made using NaOH (reagent grade) dissolved in Type 1 water. OFP copper samples were cathodically polarized for 24h at −750, −900, −1100, and −1300 $mV_{(SCE)}$ using a Solartron Analytical Modulab XM MTS potentiostat. Samples were rinsed with Type 1 water and dried in a jet of argon gas, with hydrogen measurements taking place less than 5min following the end of the polarization period. Hydrogen concentrations within OFP copper samples were measured via inert gas fusion (IGF) using a Bruker G8 GALILEO, which utilizes melt extraction to quantify the total hydrogen content via thermal conductivity, and has a detection limit of 0.01 ppm and a precision of ±0.05 ppm. IGF analysis was performed on the four samples that had been cathodically polarized at four different potentials, as well as two

controls: an OFP copper sample analyzed immediately following annealing at 900 °C to off-gas any hydrogen initially present, and a sample analyzed following both annealing and surface preparation.

In situ measurements on the copper-titanium thin film by NR and EIS.—A thin-film copper-titanium sample was cathodically charged in a mildly alkaline deoxygenated saline solution and in situ NR and EIS were performed to study hydrogen absorption into the copper. Electron-beam physical vapour deposition (EBPVD, Angstrom Engineering) was used to deposit a 4 nm film of titanium (Angstrom Engineering, 99.995%) followed by a 50 nm film of copper (Kurt Lesker, 99.99%) onto 100 mm diameter, 6 mm thick polished silicon slabs ((111), Wafer World). The EBPVD device automatically verified the thickness of the coating by quantifying the mass added to the device using an internal quartz crystal microbalance (QCM). The choice of 6 mm thick slabs was to prevent the bending of the sample during NR measurements as well as to transport the neutron beam through the silicon. The copper-titanium thin film sample was used as the working electrode in a three-electrode electrochemical cell that allowed for NR measurements to be conducted in situ. A diagram of this cell is shown in Fig. 1. An electrical connection to the copper coating was made using a pure copper ribbon tucked under the butyl rubber O-ring used to create a seal between the polytetrafluoroethylene body of the cell and the copper-titanium thin-film sample (65.22 cm^2 of copper was exposed to the electrolyte solution). A saturated Ag/AgCl reference electrode (45mV vs SCE) was used, along with a platinum plate counter electrode; nevertheless, we have translated all potential values reported in this paper to the SCE scale. The electrolyte was a pH 9 0.1M NaCl solution that was sparged with pure argon before and during the experiment. The sample was stored within a desiccator when not in use.

Electrochemical measurements were performed using an Autolab PGSTAT204 equipped with the EIS module (Metrohm). Upon addition of the argon-sparged electrolyte, a potential of −444 mV_{SCE} was applied to prevent corrosion of the copper film. The potential was lowered stepwise in succession from −444 to −1000, −1100, −1200, and −1300 mV_{SCE} with each potential being held for around 5 to 6h, except for −1300 mV_{SCE} which was held for 27h, for a total experimental time of 55h. EIS measurements were performed in triplicate continuously throughout the experiment, with current measurements made in between.

The neutron reflectometry (NR) measurements were performed at the ROG Neutron Reflectometer of the Reactor Institute Delft, Delft University of Technology, The Netherlands. The double-disc neutron beam chopper was set to a frequency of 17.7 Hz with an inter-disc distance of 0.280 m, resulting in a wavelength resolution of $\Delta\lambda/\lambda \approx 2.5\%$. The incident angle was set to 13 mrad, with the spectrum between $0.13 < \lambda < 1.3$ nm leading to a Q-range of $0.14 < Q < 1.2\ nm^{-1}$. A first slit of 1.8 mm and a second slit of 1.2 mm were used; the latter was positioned approximately 150 mm from the sample, resulting in a beam footprint of $80 \times 40\ mm^2/95 \times 40\ mm^2$ (umbra/penumbra) and a resolution of $\Delta Q/Q \approx 0.045\%$. Neutrons specularly reflected from the sample surface were detected using a ^{3}He detector. The NR data were fitted using GenX 3.6.3 to obtain estimates for the thickness, scattering length density, and roughness of each layer.[24] In the fits, the roughness of the Ti and Si substrate were kept constant. The density of the substrate and of the H_2O were kept fixed at their respective theoretical values. NR measurements were made both before the introduction of the electrolyte solution and at every hour throughout the experiment.

Rutherford backscattering spectroscopy (RBS) measurements.—RBS was performed on the aforementioned thin-film copper-titanium sample following the NR/polarization experiment to verify thickness homogeneity and identify the presence of any impurities, except for hydrogen. RBS was performed at the Western Tandetron accelerator facility using a 1 MeV He^+ beam, normal geometry, with the Si barrier detector mounted at 170°, in Cornell geometry.[25] The energy of the incident ions decreased as a result of several factors, including elastic or inelastic collisions.[26] RBS spectra were analyzed by assigning energies to the channels of the multi-channel analyzer, using an antimony-implanted calibration standard as a reference (4.93×10^{15} Sb at./cm^2). The thickness of the titanium and copper layers and the presence of impurities within those layers were determined by measuring the areal and atomic densities of these elements at the near-surface of the sample.[27] Three different spots on the surface were tested with RBS to determine the homogeneity of the deposited layers. The differences in the integrated area under the peaks were less than 4.4% for titanium, 0.7% for copper and 3.4% for platinum for each spot (below the experimental uncertainties for RBS). The appearance of trace platinum impurities on the surface of the copper is due to the anodic polarization and slight dissolution of the platinum counter electrode, followed by reduction on the copper. The Stopping Range of Ions in Matter (SIMNRA) program was utilized for fitting RBS spectra, and the near-surface profiles of the elements were accurately generated.[28] The statistical uncertainty of the resultant spectra as a function of depth is well-known and was taken into account when the profiles were simulated using SIMNRA.

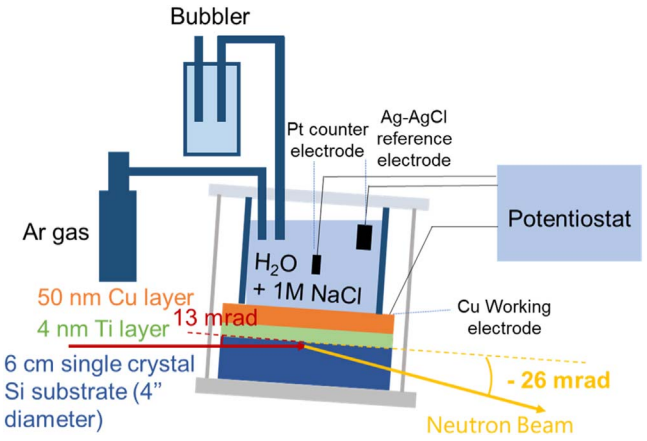

Figure 1. A diagram of the electrochemical cell used for the in situ NR experiments.

Results

Hydrogen measurements in cathodically polarized OFP copper.—Hydrogen concentrations within the OFP copper samples that had been polarized at various potentials in the electrolyte solution, measured using inert gas fusion (IGF), are presented in Table I.

Hydrogen concentration results for sample 1 indicate that the initial annealing of the OFP copper was successful in off-gassing all hydrogen, as the results of the IGF analysis were below the detection limit of 0.01 ppm. In contrast, IGF results indicate that the surface preparation procedure (polishing with SiC, water sonication, methanol sonication, water sonication, and drying in argon) increased the concentration of hydrogen slightly, absent any electrochemical polarization (sample 2). This increase in hydrogen concentration may be due to exposure of freshly abraided copper to methanol and water, resulting in some adsorption of hydrogen to copper. Thus, the similar concentrations of hydrogen recorded for OFP copper samples polarized at −750, −900, and −1100 $mV_{(SCE)}$ are likely not a result of the 24h of polarization but rather the surface preparation performed prior to polarization (samples 3–5). Furthermore, the precision error for IGF analysis of hydrogen is ±0.05 ppm, close to the range of hydrogen concentrations recorded for samples 2–5. Conversely, the hydrogen concentration measured from the OFP copper sample polarized at −1300 $mV_{(SCE)}$ (sample 6) was 0.52 ppm, suggesting that the concentration increased due to the polarization. These results imply that in mildly alkaline

Table I. H concentration values as measured from OFP copper samples via IGF analysis.

Sample #	Sample preparation	Potential (mV vs SCE)	H concentration
1	Annealed at 900 °C	NA	<0.01 ppm
2	Annealed at 900 °C, then surface preparation	NA	0.30 ppm
3	Annealed at 900 °C, then surface preparation	−750 for 24h	0.28 ppm
4	Annealed at 900 °C, then surface preparation	−900 for 24h	0.35 ppm
5	Annealed at 900 °C, then surface preparation	−1100 for 24h	0.23 ppm
6	Annealed at 900 °C, then surface preparation	−1300 for 24h	0.52 ppm

deoxygenated saline solution, cathodic polarization only increases the concentration of absorbed hydrogen in OFP copper at potentials lower than -1100 $mV_{(SCE)}$.

Current and EIS results from the cathodicaly polarized copper-titanium thin film.—Simultaneous with NR measurements, current measurements and EIS spectra were collected during the cathodic polarization experiment of the copper-titanium thin-film sample. Figure 2 shows the current density measurements plotted alongside the applied potential as a function of time. Additionally, corrosion of the copper coating was visually noted on a small portion of the working electrode after 55h, as indicated in Fig. 2 (note that the sample was not visually monitored during the period between 30 and 55 h). Figure S-1 is an optical image of the copper-titanium thin film sample following cathodic polarization and RBS measurements showing that corrosion occurred beneath the O-ring, possibility due to the ineffectiveness of argon sparging near the O-ring (see Supplemental material). However, the rest of the Cu exposed to the electrolyte retained a mirror finish (see Fig. S-1). Compared to the total working surface area, the corroded area was a minor fraction and did not affect the experimental conclusions.

Current measurements show a cathodic current flowing throughout the experiment (see Fig. 2). The small cathodic current observed at $E = -444$ mV_{SCE} may be due to the reduction of copper surface oxides. Decreases in applied potential resulted in a momentary increase in the magnitude of the cathodic current before a return to a smaller, nearly constant value. Currents measured at $E = -1000$ and -1100 mV_{SCE} became slightly more cathodic over the time these potentials were applied, suggesting that the HER proceeded more readily. In contrast, current measurements made at $E = -1200$ and -1300 mV_{SCE} continued to decrease in magnitude over the time these potentials were applied. This decrease in magnitude may have resulted from the net offsetting effect of a small anodic current induced by corrosion, which could explain the corrosion observed after 55h of the cathodic polarization experiment.

EIS spectra were also collected throughout the cathodic polarization experiment, with Nyquist plots from select but representative spectra shown in Fig. 3. It can be observed that the impedance decreased by an order of magnitude when the potential was decreased from -444 to -1000 mV_{SCE}, corresponding with HER initiation. The trend of decreasing impedance continued as the potential was decreased but reversed while the potential was held at -1300 mV_{SCE}, with the increase in impedance at the higher frequencies possibly due to corrosion buildup between the copper foil and the copper film. The Nyquist plots are slightly depressed towards the real axis, as they consist of two heavily overlapping capacitive loops corresponding with atomic hydrogen production/adsorption followed by the electrochemical recombination steps of the HER,[29–31] shown in Reactions 1 and 2, respectively:

$$H_2O_{(l)} + Cu + e^- \leftrightharpoons OH^-_{(aq)} + CuH_{(ads)} \quad [1]$$

$$CuH_{(ads)} + H_2O_{(l)} + e^- \leftrightharpoons Cu + OH^-_{(aq)} + H_{2(g)} \quad [2]$$

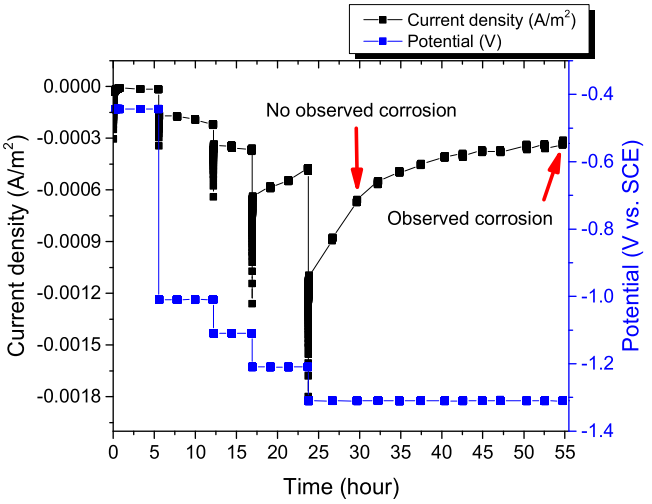

Figure 2. Current density measured and potential applied as a function of time from the copper-titanium thin film sample as a function of exposure time. Red arrows indicate points during the experiment when no corrosion was observed, and when corrosion was observed under and adjacent to the O-ring.

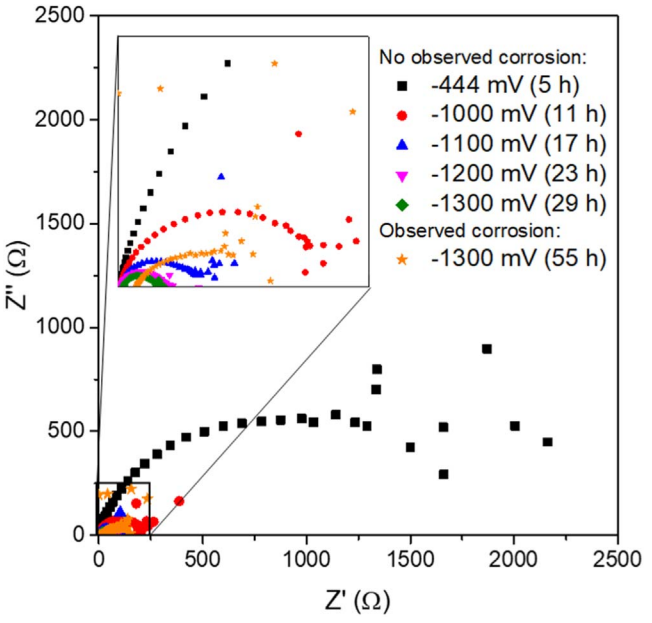

Figure 3. EIS spectra (Nyquist plots) collected at the potentials indicated around every 6h and at the end of the 55-h experiment, with observations of corrosion of the copper under and adjacent to the O-ring indicated. The inset shows an expansion of the low-impedance region.

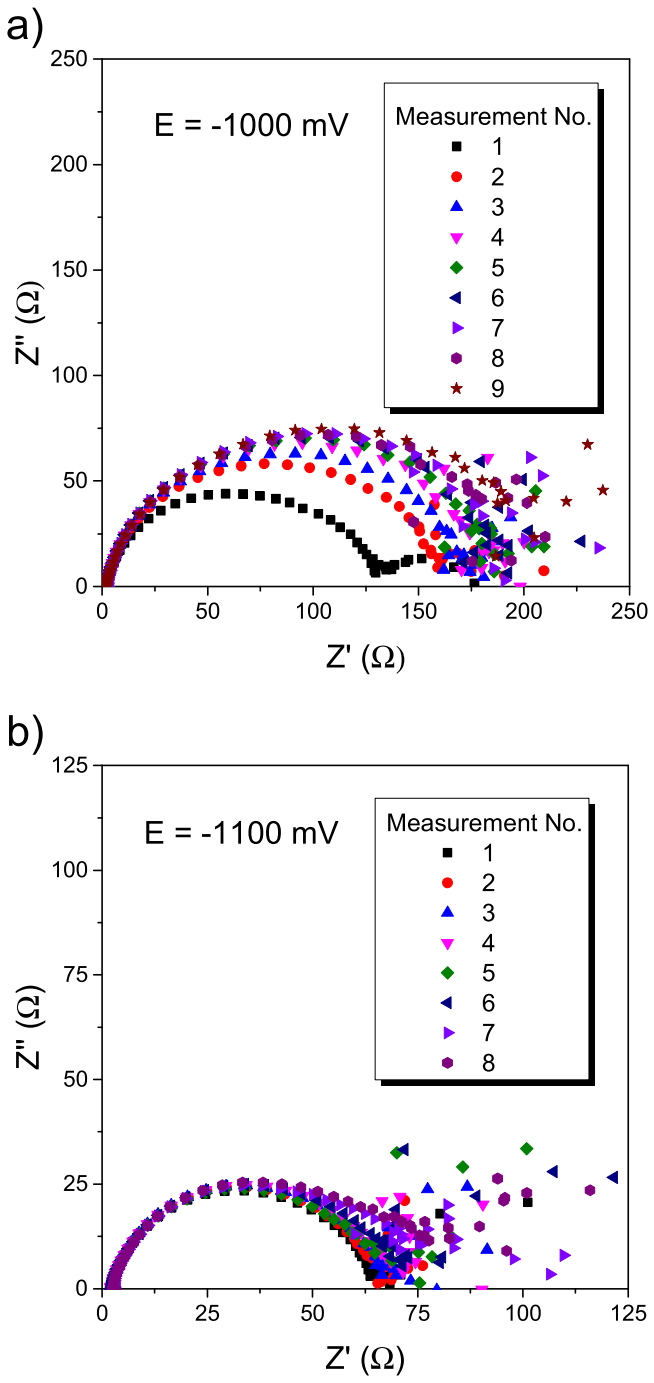

Figure 4. Nyquist plots for sets of consecutive EIS measurements during the NR scans at a) E = −1000 mV_{SCE}, and b) E = −1100 mV_{SCE}.

Additionally, hydrogen recombination can occur non-electrochemically through Reaction 3. Furthermore, any delay in recombination provides the chance for the adsorbed hydrogen to absorb and diffuse into the copper (see Reaction 4).

$$2CuH_{(ads)} \leftrightharpoons 2Cu + H_{2(g)} \quad [3]$$

$$CuH_{ads} \leftrightharpoons CuH_{abs} \quad [4]$$

Nyquist plots of EIS spectra collected when the potential was held at −1000 and −1100 mV_{SCE} are shown in Fig. 4. The low-frequency impedances at E = −1000 mV_{SCE} were higher than those measured at −1100 mV_{SCE}, which is attributed to an increase in the rate of the HER at E = −1100 mV_{SCE}. Furthermore, the low frequency impedances observed at −1000 mV_{SCE} show a trend to higher values over time, with a larger increase observed between measurements 1 and 4. In contrast, there was only a slight increase over time in the low frequency impedance observed at −1100 mV_{SCE}. This initially lower impedance when the potential was set to −1000 mV_{SCE} may indicate a higher availability of H_{ads} sites on the copper surface, promoting Reaction 1. This greater availability of sites could support either an increase in hydrogen recombination (Reactions 2 and 3) or the absorption of H_{ads} into the copper matrix.

NR results from the cathodically polarized copper-titanium thin film.—NR results from the cathodically polarized copper-titanium thin film were collected from the copper-titanium thin film sample both before and after adding the pH 9, 0.1 NaCl M argon-sparged electrolyte (Fig. S-2a). A potential of −444 mV_{SCE} was applied in the latter case to prevent corrosion of the copper, while at the same time remaining above the threshold for the HER to occur, thus avoiding hydrogen absorption into the metal.

NR is a technique that can be used to probe the thickness, composition and roughness of flat layers with a thickness of 1 to several hundreds of nanometers. It measures the reflectivity of neutrons by a sample as a function of momentum transfer vector Q, where,

$$Q = \frac{4\pi}{\lambda} \sin\theta \quad [5]$$

giving Q in units of inverse length, where θ is the incidence angle of neutrons on the specimen surface, and λ is the de Broglie wavelength of the incident neutrons. The reflectivity data are usually visualized in a reflectogram (Fig. S-2a), which displays the normalized reflectivity, being the number of reflected neutrons/number of incident neutrons, as a function of Q. The reflection of the beam of coherent neutrons from each of the interfaces in multilayer samples produces a pattern of constructive and destructive interference at the detector. Whereas the spacing of the periodic fringes on reflectograms depends on the thickness of the layers in the specimen, the amplitude of the fringes is determined by the roughness, density, and isotope-specific elemental composition of these layers. The composition also determines the critical momentum transfer vector below which total external reflection of the neutron beam occurs. Fitting the measured reflectometry data to a model yields a scattering length density (SLD) profile, showing for each layer the thickness, roughness, and SLD. The nuclei-specific nature of NR arises from changes in the scattering power of different nuclei with which the neutrons interact, as represented by the coherent neutron scattering length, which differs by element and isotope. The SLD combines the effect of the scattering length (a proxy for the composition) and the density of nuclei and is defined as,

$$SLD = \sum_i N_i b_i \quad [6]$$

where N_i is the atomic number density and b_i is the coherent neutron scattering length of isotope i. Thus, a determination of SLD by NR provides information about the composition of each layer probed in a sample, convoluted with the layer's density. As the scattering length of hydrogen is strongly negative (−3.7 fm), neutron reflectometry is particularly sensitive to the presence of hydrogen in a layer, as this leads to a strong drop of the SLD.[32]

Fits to the NR data resulted in the SLD profile displayed in Fig. S-2b, which reveals that the SLDs used for all model components were within 1% of their theoretical values. Most importantly, the SLD values of the titanium and copper layers were unaffected by the addition of water to the electrochemical cell, with the only significant difference in the SLD profile being that the ambient medium was changed (air vs H_2O). This confirms that applying a potential of −444 mV_{SCE} did not result in the hydrogenation of the

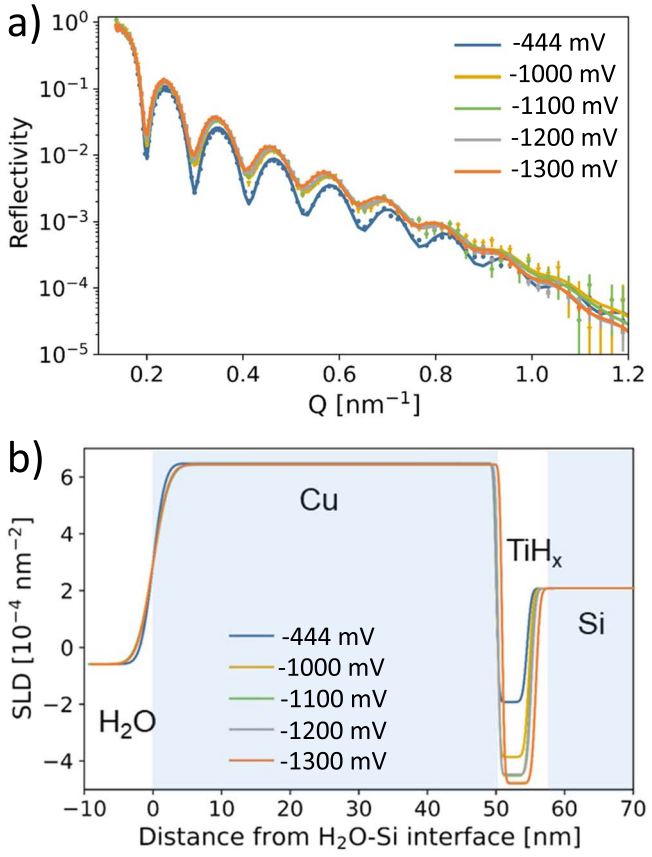

Figure 5. Neutron reflectometry results on the copper-titanium thin films at each potential (vs SCE). (a) shows the neutron reflectograms, where the points represent the measured data and the continuous curves the model fit to the data; the corresponding scattering length density profiles are displayed in b).

sample. Subsequent decreases in the applied potential lowered the potential below the threshold for the HER, resulting in hydrogen generation on the surface of the copper thin film and the evolution of bubbles from the surface. The average NR pattern collected after 1–7h of polarization at each potential, the model curve fits, and the associated SLD profiles are shown in Fig. 5. The most significant change was a lowering of the SLD of the titanium layer (see Fig. 5b). As the scattering length of hydrogen is negative, and the only nuclei with negative scattering length present in the system were hydrogen and titanium, the drop in the SLD indicates the hydrogenation of the titanium layer. The conversion of depressed SLD values to hydrogen concentration has previously been described by Bannenberg et al.[33]

In addition to hydrogen absorption into the titanium layer, we observed the slight expansion of the copper layer (by 11Å) at E = −1000 mV_{SCE} or lower (which is low enough for the HER to occur). Figure 6a shows the thickness of the copper layer and the concentration of hydrogen in the titanium layer, both plotted alongside the applied potential as a function of time. The 11Å increase in the thickness of the copper may be due to the absorption of hydrogen below the detection limit of NR (2at%), or to a slight oxidation of the copper surface. Most importantly, it can be observed from Fig. 6b that once the potential was decreased from −444 to −1000 mV_{SCE}, the hydrogen concentration in the titanium layer rapidly rose from being below the detection limit of NR up to almost a 1:1 ratio with titanium after 6h at −1000 mV_{SCE}. Subsequent decreases in the potential to −1100, −1200, and −1300 mV_{SCE} resulted in average titanium layer compositions of approximately $TiH_{1.3}$, $TiH_{1.4}$, and $TiH_{1.5}$, respectively. The variations observed in the value of x in TiH_x while the potential was held at −1100, −1200, and −1300 mV_{SCE} are not considered to be indications of a changing

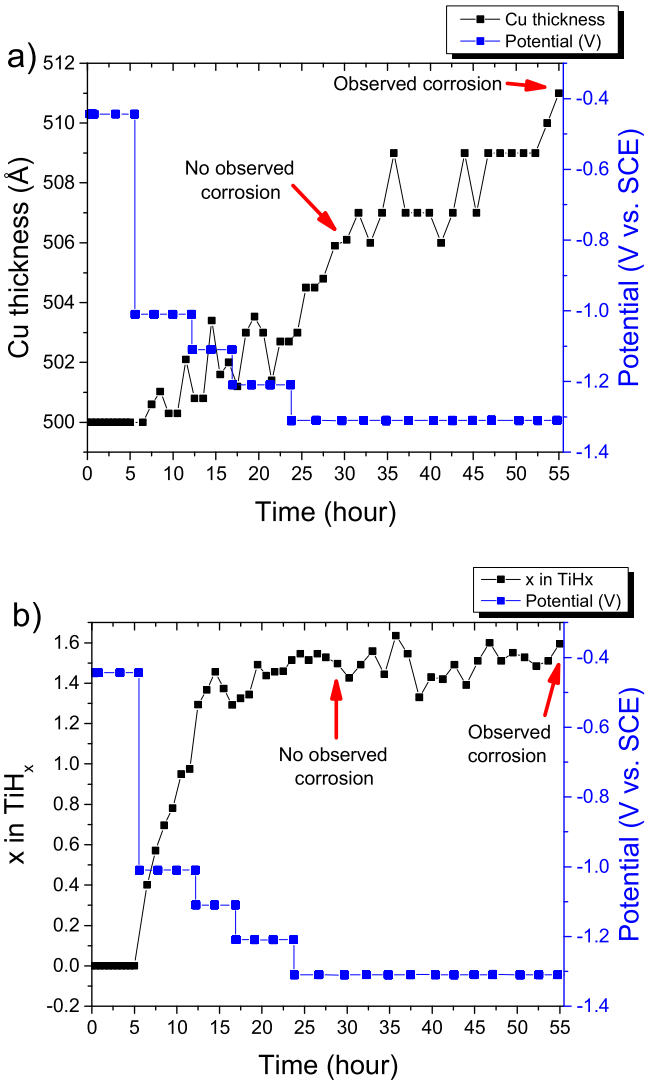

Figure 6. (a) the thickness of the Cu layer and (b) the value of x in TiH_X based on model fitting of NR data, plotted vs time and potential.

concentration of hydrogen in the Ti layer but rather statistical in nature, arising from the fitting process. From these results, it can be concluded that hydrogen diffusion occurred rapidly through the copper film into the titanium film when the electrode was polarized to potentials low enough to facilitate the HER. However, this diffusion was driven by the formation of TiH_X, and once the concentration of hydrogen had reached a steady state in the titanium layer, hydrogen diffusion through the copper film terminated. No evidence was observed for hydrogen buildup in the copper film, copper delamination from the titanium film, nor blistering of the copper film, although the slight increase in the thickness of the copper suggests hydrogen may have absorbed into the copper to a level below the detection limit of NR.

Post-cathodic polarization RBS results.—In order to elucidate compositional changes following the NR/polarization experiment of the thin copper-titanium sample, RBS measurements were performed (ex situ). Figure 7a shows RBS spectra for the Cu/Ti/Si (001) sample after cathodic polarization, with three different spots analyzed, 50 mm apart from each other. RBS indicated the presence of Ti, Cu and Pt. Differences in the integrated areas under the titanium, copper and platinum peaks were less than 4.4% for Ti, 0.7% for Cu and 3.4% for Pt for three different spots; these uncertainties are comparable to or below experimental uncertainties

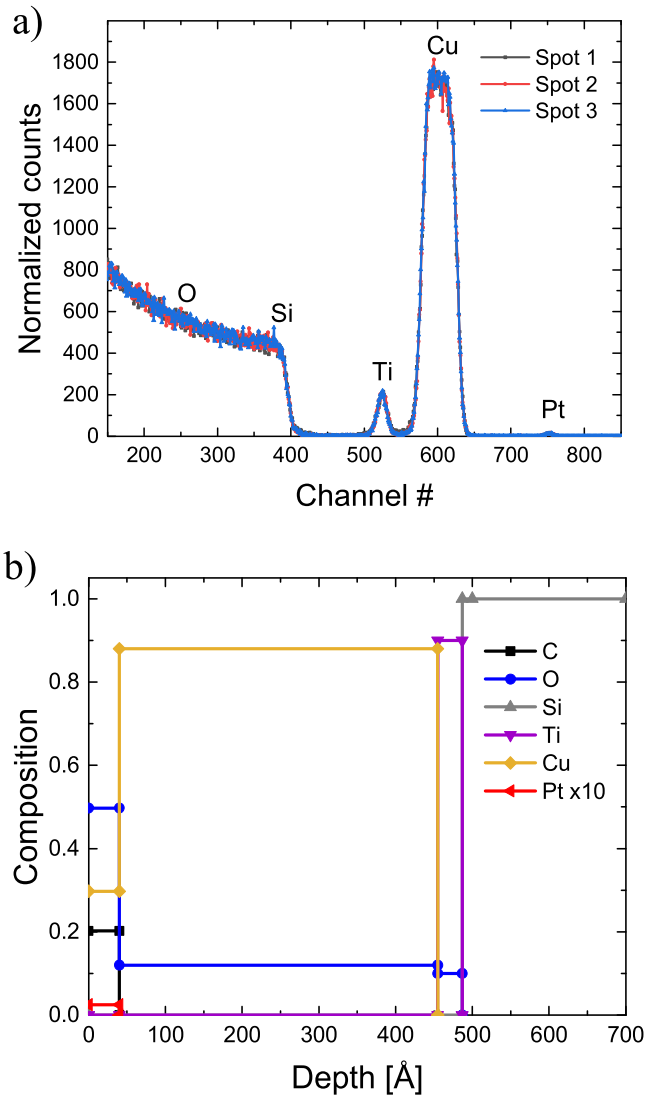

Figure 7. (a) RBS spectra collected from three spots on the copper-titanium thin film sample following cathodic polarization. (b) calculated depth profile of the copper-titanium thin film sample (40Å-$Pt_{0.0025}CuO_{0.5}C_{0.2}$ / 447Å-$CuO_{0.12}$ / 32Å-$TiO_{0.1}$ / Si(001)).

for RBS analysis.[27,34] SIMNRA fits of experimental spectra collected after cathodic polarization were performed, and the best depth profile is shown in Fig. 7b, with an overall layered stack that can be described as 40 Å $Pt_{0.0025}CuO_{0.5}C_{0.2}$ / 447 Å $CuO_{0.12}$ / 32 Å $TiO_{0.1}$ / Si(001). The presence of platinum was likely due to the anodic polarization of the platinum counter electrode. A second, identically prepared thin copper and titanium sample was also analyzed as a control sample (i.e., no polarization performed); it had a similar composition, except for the absence of Pt and a smaller oxygen fraction in the copper and titanium layers: 477 Å $CuO_{0.05}$ / 42 Å $TiO_{0.1}$ / Si(001). The presence of oxygen was not expected from our deposition conditions, with both copper and titanium targets being 99.99% pure. However, it is not surprising, as Ti is well known for its oxygen, carbon and hydrogen-gettering abilities[35] in vacuo. Including both platinum and copper peaks produced the best model fits when both elements were present on the top surface, indicating either alloying or formation of two-dimensional platinum islands.

Discussion

While the probability that UFCs will fail as a result of hydrogen absorption is deemed to be extremely low, there is an ongoing effort to gain an improved mechanistic understanding of the movement of hydrogen through the copper coating.[3] Previous studies examining the absorption of hydrogen into copper via cathodic charging have used aggressive conditions, such as the addition of the recombination poison $NaAsO_2$.[7,8] As(III) has long been known to promote hydrogen absorption into copper (see Reaction 4) by limiting the hydrogen recombination steps of the HER (see Reactions 2 and 3).[10,36] In the first portion of this study, it was demonstrated that, in the absence of a hydrogen recombination inhibitor such as As(III), hydrogen absorption into OFP copper was not observed using ex situ hydrogen analysis until a potential of -1300 $mV_{(SCE)}$ was applied. While -1300 $mV_{(SCE)}$ is lower than the potential that the surface of copper is expected to experience as a result of HS^- exposure or radiolysis in a DGR, this result demonstrates that the rate of the HER is high enough at -1300 $mV_{(SCE)}$ to offset the effects of off-gassing of hydrogen and hydrogen recombination. This result will inform future studies utilizing cathodic charging to study hydrogen absorption into copper. Moreover, it also suggests a similar approach could be used to study the absorption of hydrogen into copper via water radiolysis, where samples are exposed to gamma-radiation at varying dose rates (Gy/h) to determine the threshold for hydrogen absorption. Such a study would build off of the work of Lousada et al., who studied the absorption of hydrogen into copper via water radiolysis at a fixed gamma-radiation dose rate of 486Gy/h.[6] Similarly, this proposed study would involve varying the dose rate from $\sim$1 to 0.01Gy h^{-1} (the expected dose rate range at the Canadian UFC surface) in order to determine if the rates of hydrogen absorption into copper via water radiolysis exceed the rate of off-gassing of hydrogen from copper. The ex situ hydrogen analysis presented herein demonstrates that in the absence of recombination inhibitors like As(III), the rate of hydrogen generation needs to be vigorous to overcome the competing effects of off-gassing of hydrogen and hydrogen recombination.

The second portion of this work utilized NR and EIS to study the absorption and movement of hydrogen through copper and into titanium in situ, under cathodic polarization. This approach allows for the concentration of hydrogen in both the copper and the titanium to be monitored with precise depth sensitivity (on the order of Å) while also monitoring the HER and other electrochemical processes occurring on the surface of the copper. The absorption of hydrogen by titanium under cathodic conditions is well studied, including previously by in situ NR-EIS.[18,19] The change in the SLD of the titanium layer (see Fig. 5) indicates that hydrogen rapidly diffused through the copper layer into the titanium layer when the potential was decreased from -444 to -1000 mV_{SCE} (see Fig. 5). The hydrogen content in the titanium layer was observed to increase to $TiH_{0.4}$ within an hour after the potential was changed to -1000 mV_{SCE}, representing the greatest increase in hydrogen content in the titanium. Simultaneously, the EIS spectra collected while the potential was held at -1000 mV_{SCE} show an increase in the low-frequency impedance (see Fig. 4a); the rise in impedance suggests a decrease in the HER rate, possibly as a result of surface sites necessary for Reaction 1 becoming blocked. The concentration of hydrogen in the titanium was observed to reach a steady state upon further decreases in potential, with the concentration of hydrogen reaching $TiH_{1.5}$ at applied potential -1300 mV_{SCE}.

Despite the increase in hydrogen concentration within the titanium layer, no change was observed in the SLD of the copper layer, indicating that there was no increase in hydrogen above the 2at % detection limit for hydrogen in copper using NR. Furthermore, there were no results to indicate any other modifications to the copper layer due to hydrogen absorption (e.g., void formation, blistering, or debonding -these would have destroyed the reflectivity of the specimen surface and would therefore have been easily detected).

While no buildup of hydrogen was observed in the copper layer, it is still possible to calculate the portion of electrochemically generated hydrogen through the HER that diffused through the copper into the titanium (i.e., an "absorption efficiency"), which may

be helpful as a conservative estimate for an upper limit to the portion of hydrogen that may diffuse through the copper as a result the HER from the corrosion of copper by HS^-. The largest increase in hydrogen absorption into the titanium was measured 1h after the potential was changed from -444 mV_{SCE} to -1000 mV_{SCE}, and the composition was calculated to be $TiH_{0.4}$. This ratio of hydrogen to titanium can be used to calculate the amount of hydrogen present in the titanium layer. Based on a titanium layer thickness of 45Å and a density prior to hydrogen absorption of 4.5gcm^{-3} (measured by NR), 1.3 μmol of hydrogen diffused through the copper layer into the titanium within the first hour of polarization at $E = -1000$ mV_{SCE}. During that same one-hour time period, 41.0 μmol of hydrogen atoms were produced, assuming the entirety of the -1.16 μA of current could be attributed to hydrogen production. Thus only 3.2% of the produced hydrogen was absorbed into the copper. This value should be considered extremely conservative, due to the hydrogen gettering of the titanium layer acting as a driving force for hydrogen absorption by maintaining a steep concentration gradient across the Cu layer. Furthermore, the potential of -1000 mV_{SCE} used in this study is lower than the >-650 mV_{SCE} corrosion potential previously measured during long-term exposure of copper to HS^-.[19]

Having determined that at most 3.2% of the reduced hydrogen is absorbed into the copper, it is possible to estimate a conservative high-end concentration of hydrogen that may be absorbed into the copper coatings in the UFC. Hall et al. determined the corrosion damage that the copper coating on the UFC will experience over 1,000,000 years within the DGR, and predicted an average of 80μm and a maximum of 800μm of copper would be corroded by HS^-. Assuming the copper corroded by HS^- will form Cu_2S, the amount of hydrogen atoms produced over a 1 mm^2 area of the container would be 1.47 mmol or 14.68 mmol, if the corrosion damage to the copper coatings by HS^- is 80μm or 800μm, respectively. Hall et al. also estimated the expected and minimum predicted portion of the copper to be undamaged after 1,000,000 years to be either 2.730 mm or 1.796 mm, respectively. If 3.2% of the hydrogen atoms produced from copper corrosion by HS^- are absorbed into the undamaged copper, then the concentration of hydrogen present in the copper would increase by either 0.20 wt% or 2.98 wt% if distributed evenly throughout the expected and minimum predicted amounts of undamaged copper, respectively.

This extremely conservative estimation for hydrogen absorption into copper has a number of caveats when considering its applicability to hydrogen absorption within a DGR. For example, the buildup and morphology of corrosion products on the surface of the copper may inhibit the permeation of hydrogen into the copper. In order to obtain a more accurate measurement of hydrogen diffusion through copper, an upcoming study will be conducted to examine the absorption of hydrogen into a thin film copper-titanium sample resulting from the corrosion of copper by HS^-, rather than by cathodic charging. This upcoming research will also utilize in situ NR-EIS and will draw heavily upon the results of this preliminary study.

Conclusions

Polarization experiments were conducted in deoxygenated pH 9 0.1M NaCl solution on samples of OFP copper and a thin film sample of 500 Å copper deposited on 40 Å of titanium, with hydrogen uptake measured using IGF analysis and in situ NR-EIS, respectively. The mechanism of hydrogen absorption was discussed, and the following conclusions drawn:

1. In the absence of As(III) acting as a hydrogen recombination inhibitor, a small increase of 22 wt. ppm hydrogen was observed in OFP copper after 24h at $E = -1300$ mV(SCE), with no observed increase at $E = -1100$ mV(SCE) or higher. This result may be used to inform future cathodic charging experiments without the need for a hydrogen recombination inhibitor.
2. In situ NR-EIS experiments detected no increase in hydrogen within the copper layer of the copper-titanium thin film following 55h of polarization at potentials ranging from -444 mVSCE to -1300 mVSCE. This result supports the prediction that hydrogen absorption is unlikely to lead to any failure of the copper barrier within a proposed DGR.
3. Rapid absorption of hydrogen into the titanium layer via diffusion through the copper layer was observed on the thin-film specimen at potentials corresponding with hydrogen production. The portion of hydrogen atoms produced that diffused through the copper layer was initially 3.2%, suggesting a possible upper limit for hydrogen uptake by the copper coating of the UFC. However, future research using in situ NR-EIS to study hydrogen absorption during the corrosion of copper thin films by HS^- will help to provide a more accurate estimate. Moreover, further studies on hydrogen absorption into 3 mm copper-coated steel samples are required to draw any definitive conclusions.

Acknowledgments

This work was jointly funded by the Natural Sciences and Engineering Research Council of Canada (NSERC) and the Nuclear Waste Management Organization through Alliance Grant ALLRP561193–20. We gratefully acknowledge Tim Goldhawk and Todd Simpson at the Western Nanofabrication facility for sample preparation, and Jack Hendriks for his valuable help with RBS analysis at the Tandetron Accelerator Facility. Funding for RBS was provided by NSERC Discovery Grant RGPIN-2020–06679.

ORCID

Arthur Situm https://orcid.org/0000-0002-4329-290X
Guerman Popov https://orcid.org/0009-0005-3233-5328
James J Noël https://orcid.org/0000-0003-3467-4778

References

1. D. Weisser, *Energy*, **32**, 1543 (2007).
2. J. A. Cherry, W. M. Alley, and B. L. Parker, *The Bridge on Emerging Issues in Earth Resources Engineering*, **44**, 51 (2014).
3. D. S. Hall, M. Behazin, W. Jeffrey Binns, and P. G. Keech, *Prog. Mater Sci.*, **118**, 100766 (2021).
4. R. Becker, A. Forsström, Y. Yagodzinskyy, H. Hänninen, and M. Heikkilä, *Sulphideinduced Stress Corrosion Cracking and Hydrogen Absorption in Copper Exposed t o Sulphide and Chloride Containing Deoxygenated Water at 90◦ C, in, The Swedish Radiation Safety Authority* (2020).
5. A. Forsström, R. Becker, H. Hänninen, Y. Yagodzinskyy, and M. Heikkilä, *Mater. Corros.*, **72**, 317 (2021).
6. C. M. Lousada, I. L. Soroka, Y. Yagodzinskyy, N. V. Tarakina, O. Todoshchenko, H. Hänninen, P. A. Korzhavyi, and M. Jonsson, *Sci. Rep.*, **6**, 24234 (2016).
7. Å. Martinsson and R. Sandström, *J. Mater. Sci.*, **47**, 6768 (2012).
8. Y. Yagodzinskyy, E. Malitckii, T. Saukkonen, and H. Hänninen, *Scr. Mater.*, **67**, 931 (2012).
9. H. Magnusson and K. Frisk, *Journal of Phase Equilibria and Diffusion*, **38**, 65 (2017).
10. S. Nakahara and Y. Okinaka, *Mater. Sci. Eng. A*, **101**, 227 (1988).
11. M. G. Ganchenkova, Y. N. Yagodzinskyy, V. A. Borodin, and H. Hänninen, *Philos. Mag.*, **94**, 3522 (2014).
12. F. King and M. Behazin, *Corrosion and Materials Degradation*, **2**, 678 (2021).
13. A. Hedin et al., "Supplementary information on canister integrity issues." *Swedish Nuclear Fuel and Waste Management Company* (2019).
14. M. Truschner, A. Trautmann, and G. Mori, *Berg Huettenmaenn Monatsh*, **166**, 443 (2021).
15. P. Sahiluoma, Y. Yagodzinskyy, S. Bossyut, and H. Hänninen, *J. Nucl. Mater.*, **574**, 154177 (2023).
16. J. Turnbull, M. Behazin, J. Smith, and P. Keech, *J. Nucl. Mater.*, **559**, 153411 (2022).
17. A. Hedin, A. J. Johansson, C. Lilja, M. Boman, P. Berastegui, R. Berger, and M. Ottosson, *Corros. Sci.*, **137**, 1 (2018).
18. J. Chen, Z. Qin, and D. W. Shoesmith, *J. Electrochem. Soc.*, **157**, C338 (2010).
19. J. Chen, Z. Qin, and D. W. Shoesmith, *Electrochim. Acta*, **56**, 7854 (2011).
20. W. H. Miller, A. Kumar, and W. Meyer, *J. Nondestr. Eval.*, **10**, 151 (1991).
21. J. J. Noël, *Physics in Canada*, **74** (2018).
22. M. Vezvaie, J. Noël, Z. Tun, and D. Shoesmith, *J. Electrochem. Soc.*, **160**, C414 (2013).

23. M. Guo, J. Chen, T. Martino, M. Biesinger, J. Noël, and D. Shoesmith, *J. Electrochem. Soc.*, **166**, C550 (2019).
24. A. Glavic and M. Björck, *J. Appl. Crystallogr.*, **55** (2022).
25. S. Gotoh and Z. Takagi, *J. Nucl. Sci. Technol.*, **1**, 311 (1964).
26. M. A. Brocklebank and H. Resolution, "Ion beam investigations of the mechanisms of titanium anodization, in department of physics and astronomy." (2018), The University of Western Ontario.
27. J. R. Tesmer and M. Nastasi, "Handbook of modern ion beam materials analysis." *Materials Research Society* (1995).
28. W. Chu, J. Mayer, and M. Nicolet, *Backscattering spectroscopy* (New York) (Academic, London) (1978).
29. O. Azizi, M. Jafarian, F. Gobal, H. Heli, and M. Mahjani, *Int. J. Hydrogen Energy*, **32**, 1755 (2007).
30. A. Alobaid, C. Wang, and R. A. Adomaitis, *J. Electrochem. Soc.*, **165**, J3395 (2018).
31. N. Krstajić, M. Popović, B. Grgur, M. Vojnović, and D. Šepa, *J. Electroanal. Chem.*, **512**, 16 (2001).
32. V. F. Sears, *Neutron News*, **3**, 26 (1992).
33. L. J. Bannenberg, H. Schreuders, L. van Eijck, J. R. Heringa, N.-J. Steinke, R. Dalgliesh, B. Dam, F. M. Mulder, and A. A. van Well, *J. Phys. Chem. C*, **120**, 10185 (2016).
34. Y. Wang and M. Nastasi, *Handbook of modern Ion beam materials analysis Materials Research Society* (2009).
35. L. V. Goncharova, M. Dalponte, T. Gustafsson, O. Celik, E. Garfunkel, P. S. Lysaght, and G. Bersuker, *J. Vacuum Sci.Technol. A*, **25**, 261 (2007).
36. D. W. DeWulf and A. J. Bard, *J. Electrochem. Soc.*, **132**, 2965 (1985).